Soil Dynamics and Earthquake Engineering 31 (2011) 209–222

Contents lists available at ScienceDirect

Soil Dynamics and Earthquake Engineering

journal homepage: www.elsevier.com/locate/soildyn

Performance-based earthquake early warning

Iunio Iervolino *

Dipartimento di Ingegneria Strutturale, Università degli Studi di Napoli Federico II, Via Claudio 21, 80125 Naples, Italy

ARTICLE INFO

Article history:
Received 15 April 2010
Received in revised form
21 July 2010
Accepted 26 July 2010

ABSTRACT

Significant investments are undergoing internationally to develop earthquake early warning (EEW) systems. So far, reasonably, the most of the research in this field was lead by seismologists as the issues to determine essential feasibility of EEW were mainly related to the earthquake source. Many of them have been brilliantly solved, and the principles of this discipline are collected in the so-called *real-time seismology*. On the other hand, operating EEW systems rely on general-purpose intensity measures as proxies for the impending ground motion potential and are suitable for population alert. In fact, to date, comparatively little attention was given to EEW by earthquake engineering, and design approaches for structure-specific EEW are mostly lacking. Applications to site-specific systems have not been extensively investigated and EEW convenience is not yet proven except a few pioneering cases, although the topic is certainly worthwhile. For example, in structure-specific EEW the determination of appropriate alarm thresholds is important when the false alarm may induce significant losses; similarly, economic appeal with respect to other risk mitigation strategies as seismic upgrade should be assessed. In the paper the least issues to be faced in the design of engineering applications of EEW are reviewed and some work done in this direction is discussed. The review presented intends to summarize the work of the author and co-workers in this field illustrating a possible *performance-based* approach for the design of structure-specific applications of EEW.

1. Introduction

At a large scale, the basic elements of an earthquake early warning (EEW) system are seismic instruments (individual or multiple stations arranged in form of a network), a processing unit for the data measured by the sensors and a transmission infrastructure spreading the alarm to the end users [1]. This alarm may trigger security measures (manned or automated), which are expected to reduce the seismic risk in real-time, i.e., before the strong ground motion reaches the warned site. In fact, from the engineering point of view, an EEW system may be appealing for specific structures only if it is competitive cost-wise and/or if it allows to achieve some seismic performance traditional risk mitigation strategies cannot. EEW may be particularly useful in all those situations when some ongoing activity may be profitably interrupted or posed in a safe mode to prevent losses in the case of an earthquake (i.e., a *security action* is undertaken). This is the case, for example, of facilities treating hazardous materials as nuclear power plants or gas distribution systems. In the first case, the reactor can be temporarily shut down before the earthquake hits, in the second case, distribution may be interrupted until it is verified damages and releases potentially triggering fires and explosions did not occur. In these situations it is clear that the early warning, which is in principle only a piece of *information* regarding the earthquake, represents the input for a local protection system. Simpler yet potentially effective applications are related to manned operations as surgery in hospitals or the protection from injuries due to fall of non-structural elements in buildings. EEW information seems less suitable to reduce the risk directly related to structural damage (although some potential application may be conceived, it has to be proven that they are more convenient than most traditional seismic protection systems).

Two points, not usually faced by earthquake engineering, emerge then: (i) because effective engineering applications of EEW involve shut down of valuable operations and the downtime is very costly for production facilities, unnecessary stops (*false alarms*) should be avoided as much as possible; and (ii) development of EEW applications basically deals with the *best* engineering use of seismological information provided in *real-time* on the approaching earthquake. In fact, the basic design key points for EEW applied to a specific engineering system are:

- the estimated earthquake potential on the basis of the EEW information;
- the available time before the earthquake strikes (*lead-time*); and

* Tel.: +39 081 7683488; fax: +39 081 7683491.
E-mail address: iunio.iervolino@unina.it
URL: http://wpage.unina.it/iuniervo/.

0267-7261/$ - see front matter © 2010 Elsevier Ltd. All rights reserved.
doi:10.1016/j.soildyn.2010.07.010

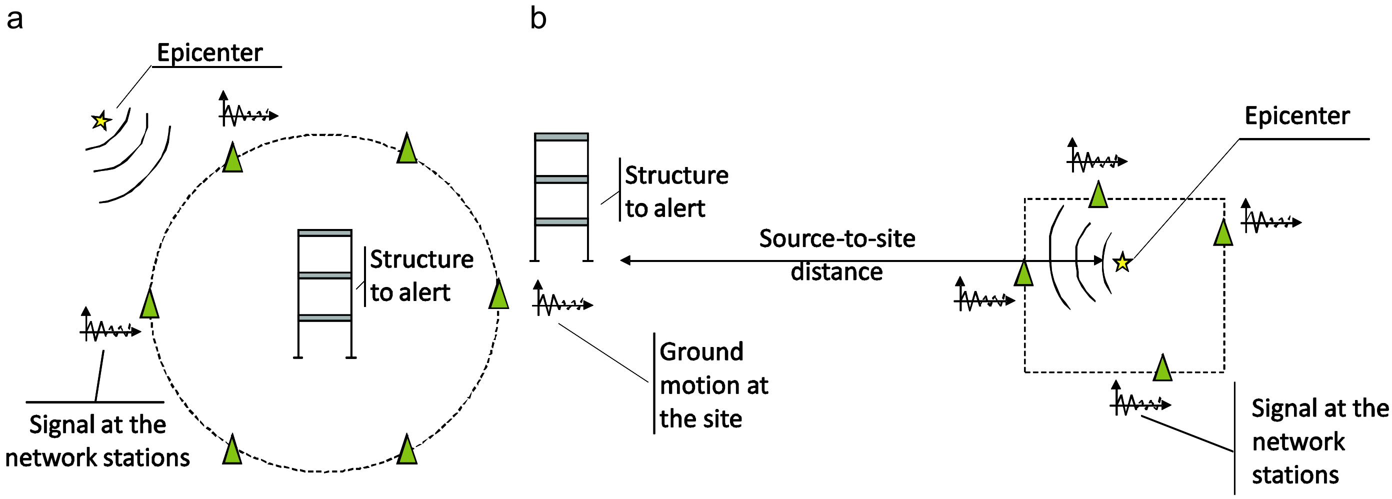

Fig. 1. Site-specific (a) and hybrid (b) EEW schemes, modified from [8].

- the system performance (proxy for the loss) associated to the case the alarm is issued, which may also include the cost of false alarm and depends on the chosen security action.

In the following, the work of the author and co-workers regarding these issues will be reviewed. It will be discussed how these three items are not independent to each other and that the whole involves very large uncertainty.

2. Estimating ground motion potential in real-time

Conceptually, EEW systems are often identified by the configuration of the seismic network, as *regional* or *site-specific* [2].

Site-specific systems are devoted to enhance in real-time the safety margin of critical systems as nuclear power plants, lifelines or transportation infrastructures by automated safety actions (e.g., [3,4]). The networks for specific EEW cover the surroundings of the system creating a kind of a fence for the seismic waves (Fig. 1a). The location of the sensors depends on the time needed to activate the safety procedures before the arrival of the more energetic seismic phase at the site (or *lead-time*). In these *seismic alert systems* [5] the alarm is typically issued when the ground motion at one or more sensors exceeds a given threshold and there is no attempt to estimate the source features as magnitude (M) and location because a local measure of the effects (i.e., the ground motion) is already available. Another type of site-specific system is the *on-site* system, in which the seismic sensors are placed within the structure to warn. In this case the ground damaging potential is typically estimated on the basis of the P-waves and the *lead-time* is given by the residual time for the damaging S-waves to arrive.

Regional EEWS' consist of wide seismic networks covering a portion of the area which is likely to be the source of earthquakes. Data from regional networks are traditionally used for long term seismic monitoring or to estimate, right after the event (i.e., in *near-real-time*), territorial distributions of ground shaking obtained via spatial interpolation of records (e.g., *Shakemap* [6]) for emergency management. Regional infrastructures are usually available in seismic regions and are operated by governmental authorities; this is why the most of the ongoing research is devoted to exploit these systems for real-time alert use (Fig. 1b) as a few examples attest (e.g., [7]). In fact, the work presented in the following mostly refers to the feasibility and design of structure-specific alert (i.e., as in site-specific systems) starting from estimating the peak ground motion at the site using the sole information from regional networks, which consists of the estimation of source features as M and location of the earthquake. This was referred to as *hybriding* the two EEW approaches [8]. Moreover, herein, an attempt to integrate on-site and regional seismic sensors for earthquake early warning is also discussed (see Section 3).

2.1. Real-time probabilistic seismic hazard analysis (RTPSHA)

In the framework of performance-based earthquake engineering or PBEE [9] the earthquake potential, with respect to the performance demand for a structure, is estimated via the so-called probabilistic seismic hazard analysis or PSHA [10], which consists of the probability that a ground motion intensity measure (IM), likely to be a proxy for the destructive power of the earthquake, the peak ground acceleration (PGA) for example, is exceeded at the site of interest during the *service life* of the structure. This is done via Eq. (1), which refers to a single earthquake source[1]: λ is the rate of occurrence of earthquakes on the source; $f(m)$ is the probability density function or PDF of M; $f(r)$ is the PDF of the source-to-site-distance (R), and $f(im|m,r)$ is the PDF of IM given M and R (e.g., from a ground motion prediction equation or GMPE).

$$f(im) = \lambda \int_m \int_r f(im|m,r)\, f(m)\, f(r)\, dr\, dm \qquad (1)$$

Because seismologists have recently developed several methods to estimate M and R in real-time while the event is still developing, for example, from limited information of the P-waves, the PSHA approach can be adapted for earthquake early warning purposes. The so-called real-time PSHA or RTPSHA, introduced in [8], tends to replace some of the terms in Eq. (1), with their real-time counterparts.

It has been shown in [11] that if at a given time t from the earthquake's origin, the seismic network can provide a vector of measures informative for the magnitude, $\{\tau_1, \tau_2, \ldots, \tau_n\}$, then the PDF of M conditional to the measures, $f(m|\tau_1,\tau_2,\ldots,\tau_n)$, may be

[1] In Eq. (1) it is assumed, for simplicity, that M and R are independent random variables, which is not the general case.

obtained via the Bayes theorem[2]:

$$f(m|\tau_1,\tau_2,...,\tau_n)=k\, e^{\left[2\mu_{\ln(\tau)}\left(\sum_{i=1}^{n}\ln(\tau_i)\right)-n\mu_{\ln(\tau)}^2\right]/2\sigma_{\ln(\tau)}^2}e^{-\beta m} \tag{2}$$

where β is a parameter depending on the Gutenberg–Richter relationship for the source and k is a constant. $\mu_{\ln(\tau)}$ and $\sigma_{\ln(\tau)}$ are the mean and standard deviation of the logs of the measure used to estimate M, respectively (e.g., from [12]). Note finally that the PDF of M in Eq. (2) depends on the real-time data only via n and $\sum_{i=1}^{n}\ln(\tau_i)$, which are related to the geometric mean, $\hat{\tau}=\sqrt[n]{\prod_{i=1}^{n}\tau_i}$.

Regarding R, because of rapid earthquake localization procedures (e.g., [15]), a probabilistic estimate of the epicenter may also be available based on the sequence according to which the stations trigger, $\{s_1, s_2,\ldots, s_n\}$. Thus, the real-time PDF of R, $f(r|s_1,s_2,...,s_n)$, may replace $f(r)$ in Eq. (1). In fact, the PSHA hazard of Eq. (1) has its real-time adaption in Eq. (3). Because when the earthquake is already occurring the λ parameter does not apply, in principle, no further data are required to compute the PDF of the IM or, equivalently, the complementary cumulative distribution (or hazard curve) of IM at any site of interest.

$$f(im|\underline{\tau},\underline{s})=\int_m\int_r f(im|m,r)\,f(m|\tau_1,\tau_2,...,\tau_n)\,f(r|s_1,s_2,...,s_n)\,dr\,dm \tag{3}$$

A simulation of the RTPSHA approach for a magnitude 6 event is given in Fig. 2 referring to the Irpinia Seismic Network (ISNet, see [19]) in Campania (southern Italy). The figure shows that because the knowledge level about the earthquake (i.e., M and R) increases as the seismic signals are processed by an increasing number of seismic sensors (i.e., n), the real-time hazard evolves with time. In Fig. 2 the panels (a), (b) and (c) show the number of stations of the network that have measured the parameter informative for the magnitude at three different instants form the earthquake origin time. In the (c) and (d) panels, the corresponding PDFs of M and R are given, while panel (e) shows the real-time hazard curves in which the IM considered is the PGA on stiff soil (computed using the GMPE of [17]). The three instants chosen correspond to when 2, 18 and 29 (the whole network) have recorded at least 4 s of the P-waves, which is the required time to estimate τ according to [12]. For further details on the simulation the reader should refer to [8,11,14].

Note finally that the RTPSHA can be easily extended to estimate in real-time the response spectrum ordinates; this has been done in [13].

2.2. Decisional rules, alarm thresholds and false alarm probabilities

An essential engineering issue in earthquake early warning is the *alarming decisional rule*, which should be based on the consequences of the decision of alarming or not and is remarkably dependent both on the information gathered on the earthquake and on the system to alarm.

If the RTPSHA is the approach used in the early warning system, the knowledge level about the earthquake at a certain time is represented by the hazard curve computed at that instant. The alarming decisional rule should be established based on that. The simplest is to alarm if the expected value of the considered IM is larger than a threshold, Eq. (4),[3] i.e., to alarm if

$$E[IM]=\int_{-\infty}^{+\infty} im\;f(im)\,d(im)\geq im_c \tag{4}$$

The im_c threshold depends on the system to alarm. For example, if structural damage is the consequence, and the IM is the PGA, the PGA_c value should reflect the ground motion intensity above which damages for that specific structure are expected, e.g., the PGA value used for the design of the structure.

A more refined decisional rule, still based on the RTPSHA outcome, may be to alarm if the critical IM value has an *unacceptable* risk (represented by the probability value $\Pr_c$) of being exceeded in that earthquake, Eq. (5), i.e., to alarm if

$$\Pr[im>im_c]=1-\int_{-\infty}^{im_c} f(im)\,d(im)\geq \Pr_c \tag{5}$$

This latter approach to the EEW alarming decision is similar to the earthquake resistant design in codes worldwide, where the design is carried out for an IM value corresponding to a fixed probability of exceedance in the lifetime of the structure (e.g., 10% in 50 years). In fact, Eq. (5) may be seen as Eq. (6), i.e., to alarm if

$$im(\Pr_c)>im_c \tag{6}$$

which means that, if PGA is the IM, the alarm has to be issued if the PGA, which in the real-time hazard curve has the critical probability of being exceeded, is larger than the critical PGA for the structure.

The two rules of Eqs. (4) and (5) are represented in Fig. 3a where, for the PDF of PGA derived from the hazard curve at $n=29$ in Fig. 2, it is shown a case in which, for the specific im_c and $\Pr_c$ values, the alarm should be issued according to the first rule and should not be according to the second one.

As discussed, the PDF of M may be seen as sole function of $\hat{\tau}=\sqrt[n]{\prod_{i=1}^{n}\tau_i}$; moreover, as shown in Section 2.4, simply the modal value of R may adequately represent its PDF due to the negligible uncertainty involved in the earthquake location rapid estimation methods. Therefore, because the GMPE is a static piece of information (not depending on the real-time measures), the RTPSHA integral may be computed offline for all possible values of the $\hat{\tau}$ and R pair, and the result has only to be retrieved in real-time without the need for computing it. This is an attractive feature of the proposed approach. As an example, in Table 1 the probabilities of exceedance are tabulated for the arbitrary PGA_c value of 0.017 g, using the GMPE of [17] and as a function of the two independent parameters required to compute the RTPSHA integral. Having them pre-computed allows to immediately check in real-time the decisional rule of Eq. (5).

The decisional rule allows to define what false (FA) and missed (MA) alarms are, i.e., if the decision, whichever it is, results to be wrong. In the case of the rule of Eq. (5) these definitions become

$$\begin{cases} MA: & \{\Pr[IM>IM_c]<\Pr_c\cap im>im_c\} \\ FA: & \{\Pr[IM>IM_c]>\Pr_c\cap im<im_c\} \end{cases} \tag{7}$$

In other words a MA [FA] occurs when the risk, the critical IM level is going to be exceeded, is too low [high] to issue [to not issue] the alarm, while the actual IM occurring at the site is higher [lower] than im_c. Consequently, false and missed alarms probabilities, P_{FA} and P_{MA}, which are dependent on the time when the decision is supposed to be taken, may be computed; see [8,14] for details. An example, referring to the simulation of Fig. 2 for some arbitrary PGA_c values and when $\Pr_c$ is equal to 0.2, is given in Fig. 3b. Two important results emerge from the plots: (1) after a certain time the probabilities stabilize; this reflects the fact that after a certain instant the information about the real-time hazard does not change anymore (see the following section); and (2) there is a trade-off, that is, one can play with $\Pr_c$ and im_c to lower P_{FA}, but this always implies that P_{MA} is going to increase and vice-versa.

[2] It is to mention that simpler approaches to estimate M can be implemented in the RTPSHA [13] although the Bayesian one has proven to be the most efficient one [14].

[3] Conditional dependencies are dropped from the equations for simplicity.

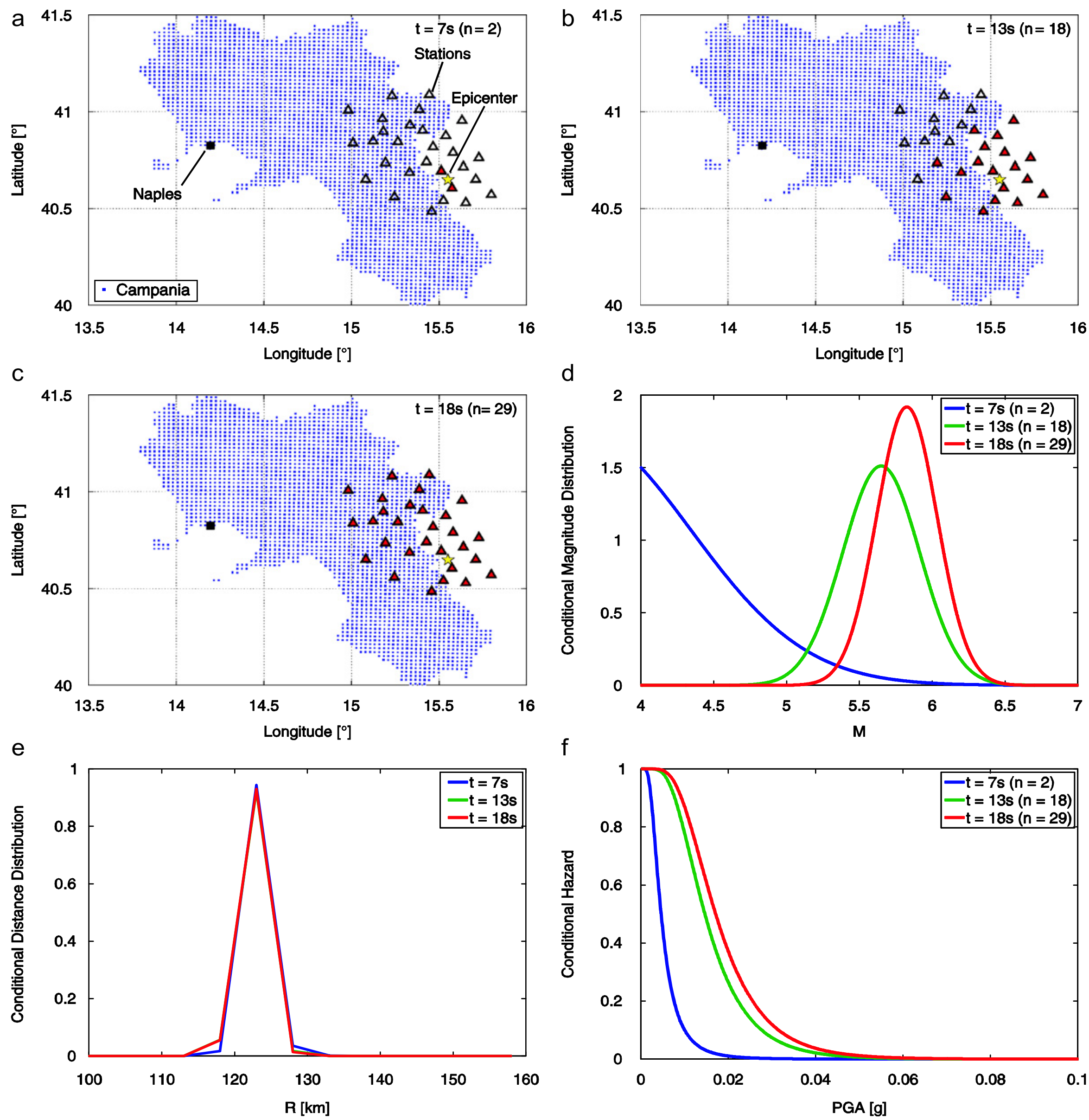

Fig. 2. (a)–(c) Seismic stations that have measured the parameter informative for the magnitude of the earthquake (i.e., 4 s of the P-wave velocity signal [12]) at three different instants during the earthquake; (d)–(f) are the *M*, *R* and *PGA* distributions computed at the same instants via the RTPSHA approach (modified from [14]).

The careful evaluation of the false alarm (or *cry wolf*) probability is increasingly important as the cost associated to the alarm, or to the following security action, raises. In fact, in those cases when the alarm has neither costs nor undesired consequences, the optimal solution is to issue the alert whenever an earthquake event is detected by the EEW system. Conversely, if the alarm may cause costly downtime or affects large communities (e.g., in the case of emergency stop of power plants or lifelines' distribution networks) the alarm decision conditions have to be carefully evaluated to prevent, in the long run, the loss related to false alarms to be unacceptably large. In Fig. 4 a simple scheme linking three important design variables of engineering earthquake early warning are shown for three different possible EEW applications (relative position with respect to the axes was arbitrarily given). In the figure it is shown that there are security actions that require a limited lead-time and have a low impact, then a larger FA rate is accepted with respect to actions affecting a larger part of the community more costly, time consuming to operate and for which, then, false alarms are less tolerable [20].

It is to mention that decisional rules based on a ground motion *IM* thresholds, as those presented, have the advantage to be simple and require limited information of the structure to alert (i.e., those required to set im_c). However, the *IM* is only a proxy for the loss associated to the earthquake hitting the structure. In fact, the alarming decision should be better taken comparing in real-time the expected losses consequent the decision to alarm or to not alarm, conditional on the available information about the impending earthquake. This has been investigated in [11] and is briefly discussed in Section 4.

2.3. ERGO—an example of RTPSHA terminal

The EaRly warninG demO (ERGO) was developed to test the potential of hybrid EEW based on RTPSHA [21]. The system was

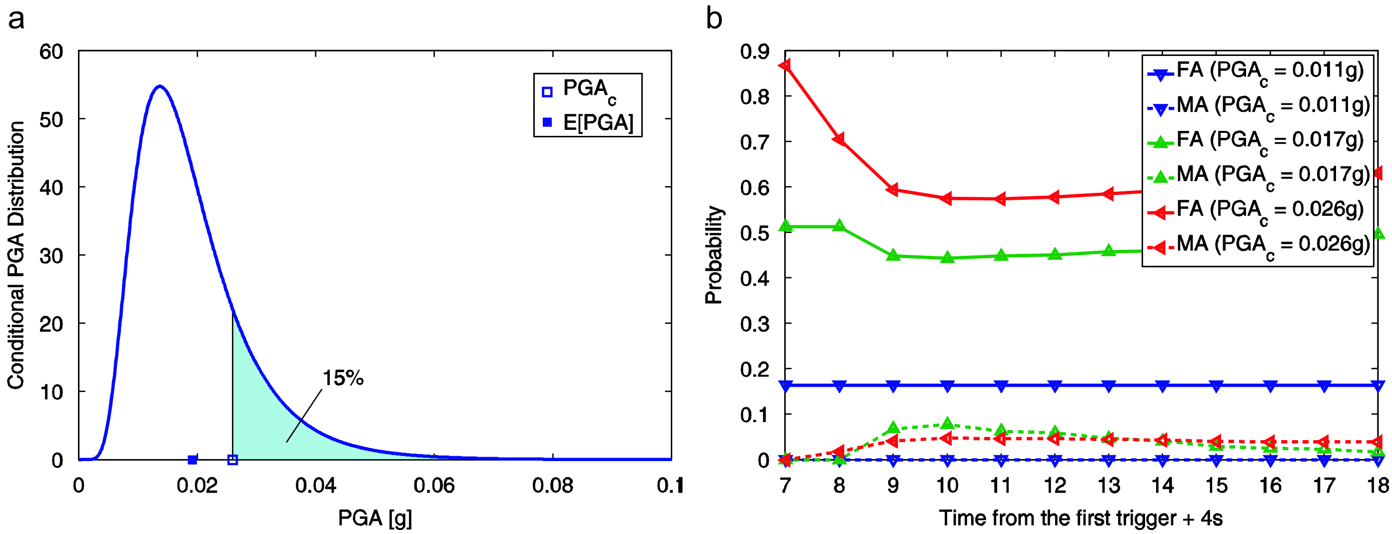

Fig. 3. Representation of decisional rules (a) and examples of false and missed alarm probabilities as a function of time for different *IM* values (b).

Table 1
Exceedance probability for an arbitrary PGA_c value of 0.017 g as a function of the only two parameters required to compute the RTPSHA integral, showing offline computability.

$n=18$	Estimated source-to-site distance, i.e., modal value of the PDF of R (km)										
$\hat{\tau}$[s]	50	60	70	80	90	100	110	120	130	140	150
0.2	0.0363	0.0136	0.0053	0.0021	0.0009	0.0004	0.0002	0.0001	0.0000	0.0000	0.0000
0.4	0.0442	0.0173	0.0069	0.0029	0.0012	0.0006	0.0003	0.0001	0.0001	0.0000	0.0000
0.6	0.1338	0.0683	0.0351	0.0184	0.0098	0.0054	0.0030	0.0017	0.0010	0.0006	0.0003
0.8	0.6085	0.4627	0.3423	0.2490	0.1795	0.1289	0.0925	0.0664	0.0479	0.0346	0.0251
1.0	0.9240	0.8563	0.7737	0.6843	0.5949	0.5102	0.4331	0.3648	0.3055	0.2547	0.2117
1.2	0.9912	0.9776	0.9548	0.9224	0.8814	0.8332	0.7801	0.7240	0.6669	0.6102	0.5552
1.4	0.9990	0.9968	0.9919	0.9833	0.9700	0.9516	0.9279	0.8992	0.8661	0.8294	0.7897
1.6	0.9998	0.9991	0.9973	0.9938	0.9875	0.9779	0.9643	0.9465	0.9245	0.8985	0.8689
1.8	0.9999	0.9995	0.9984	0.9961	0.9917	0.9847	0.9744	0.9604	0.9425	0.9207	0.8953
2.0	0.9999	0.9996	0.9988	0.9969	0.9933	0.9873	0.9783	0.9660	0.9499	0.9301	0.9068

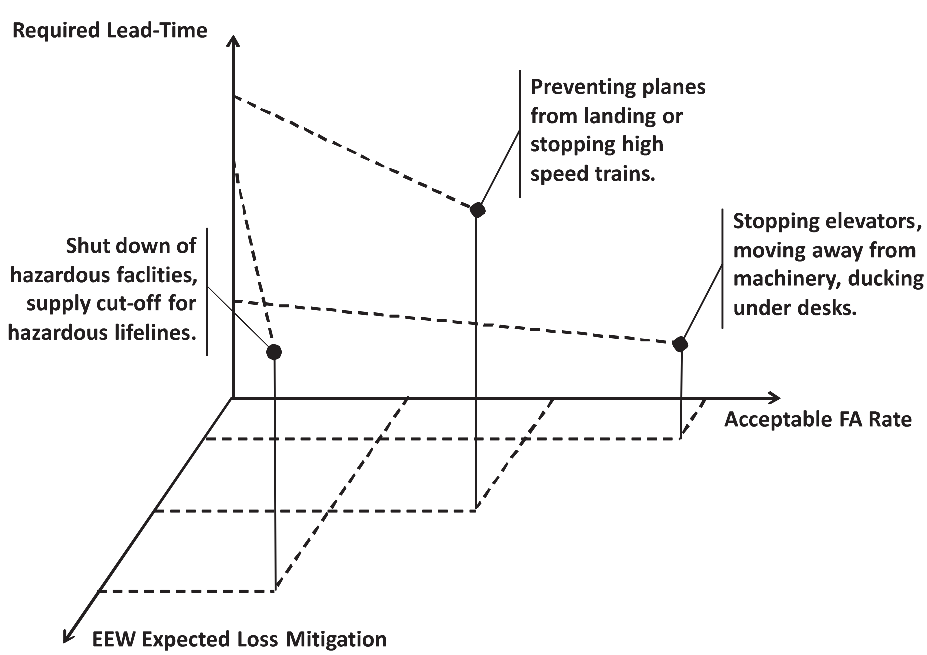

Fig. 4. Impact of missed/false alarms for categories of EEW applications, modified from [20].

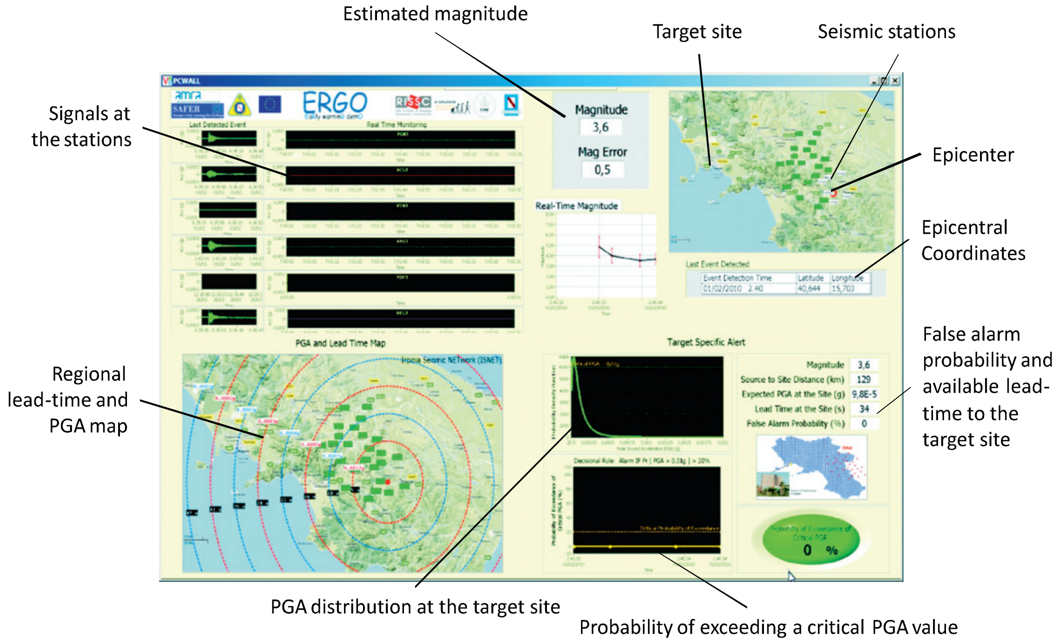

Fig. 5. ERGO, a RTPSHA-based early warning terminal.

developed by the staff of the RISSC Lab (www.rissclab.unina.it). ERGO processes in real-time the accelerometric data provided by a sub-net (6 stations) of ISNet and is installed in the main building of the School of Engineering of the University of Naples Federico II, in Naples, which is the target site of the EEW. It is able to perform RTPSHA and eventually to issue an alarm in the case of potentially dangerous events occurring in the southern Appennines region. ERGO is composed of the following four panels (Fig. 5):

(1) *Real-time monitoring and event detection.* In this panel two kinds of data are given: (a) the real-time accelerometric signals of the stations, shown on a 2 min time window; and (b) the portion of signal that, based on signal-to-noise ratio, determined the last trigger (i.e., event detection) of a specific station (on the left). Because it may be the case that local noise (e.g., traffic) determines a station to trigger, the system declares an event (*M* larger than 3) only if at least three stations trigger within the same 2 s time interval.

(2) *Estimation of earthquake parameters.* This panel activates when an event is declared. If this condition occurs, the magnitude and location are estimated in real-time as a function of evolving information from the first panel. Here the expected value of magnitude, as a function of time and the associated standard error, is given. Moreover, on a map where also the stations are located (rectangles), it shows the estimated epicenter (red circle), its geographical coordinates and the origin time.[4]

(3) *Lead-time and peak-shaking map.* This panel shows the lead-time associated to S-waves for the propagating event in the whole region. As a further information, on this panel the expected *PGA* on stiff soil is given on the same map. As per the second panel, this one activates only if an event is declared from panel 1 and its input information comes from panel 2.

(4) *RTPSHA and alarm issuance decision.* This panel performs RTPSHA for the site where the system is installed based on information on magnitude and distance from panel 2. In particular, it computes and shows real-time evolving PDFs of *PGA* at the site. Because a critical *PGA* value has been established (arbitrarily set equal to 0.01 g) the system is able to compute the risk this *PGA* is exceeded as a function of time. If such a risk exceeds 0.2, the alarm is issued and an otherwise green light turns to red, as per Eq. (5). This panel also gives, as summary information, the actual risk that the critical *PGA* value is exceeded along with the lead-time available and the false alarm probability.

Fig. 5 refers to a real event detected and processed in real-time by ERGO on February 01, 2010. The system estimated the event as an *M* 3.6, with an epicenter about 130 km far from the site. Because the event was a low-magnitude large-distance one, the risk the PGA_c could be exceeded was negligible and the alarm was, correctly, not issued. Finally, note that ERGO is a visual panel only for demonstration and testing purposes, but it may be virtually ready to be connected to devices for real-time risk reduction actions.

2.4. Uncertainties in EEW ground motion predictions and information-dependent lead-time

Three different sources of uncertainty affect the *IM* estimation according to Eq. (3), that is, those related to the estimation of *M*, *R* and *IM* given *M* and *R*. Except for the PDF of *IM* given *M* and *R*, the uncertainty involved is time-dependent because the uncertain estimations of magnitude and distance are also time-dependent. A great deal of research has focused on the fine tuning of the estimation of *M* and related uncertainty; however, in the RTPSHA ground motion prediction uncertainty, that on *M* is not the weak link. This is proven in [14] from where Fig. 6a is taken. It shows, for the *M* 6 event simulated in Fig. 2, the coefficient of variation (*CoV*, the ratio of the standard deviation to the mean) of the *PGA* prediction as the time from the origin time of the earthquake and number of stations providing τ (the information about the source parameters of the impending earthquake) increase. This may be

[4] Earthquake magnitude and location estimation methods employed by ERGO for RTPSHA purposes are based on simplified methods with respect to those mentioned in the early sections of the paper.

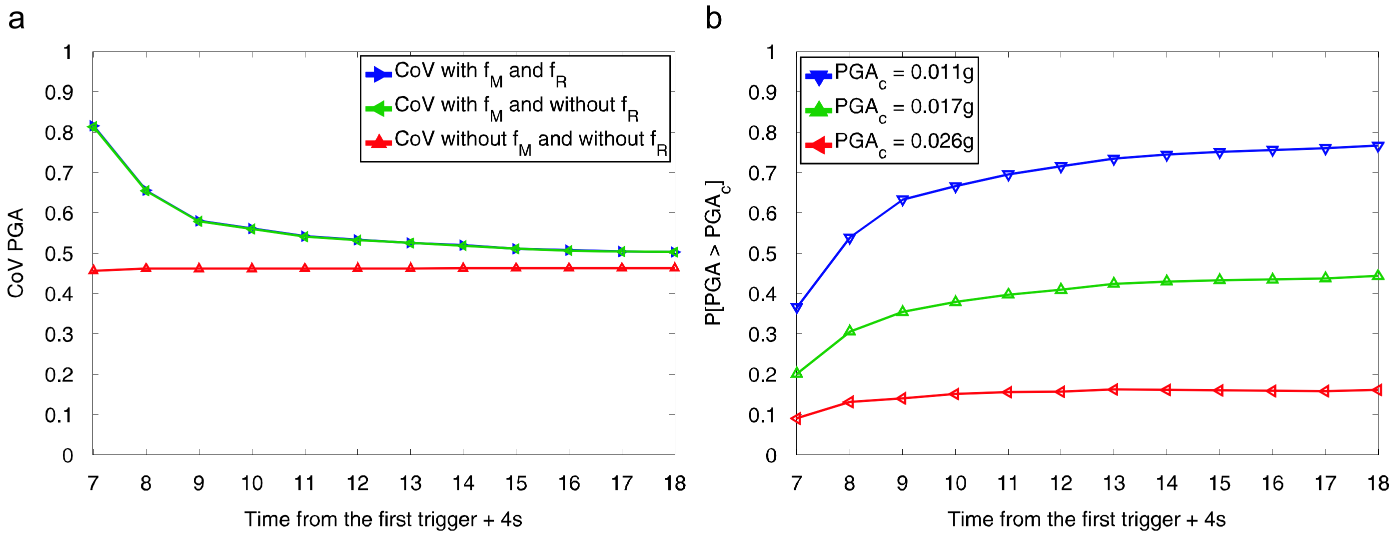

Fig. 6. Coefficient of variation of the *IM* PDFs when different uncertainties are considered (a) and dependence of *IM* estimations as a function of time (b), adapted from [14].

seen as a measure of the evolving uncertainty on EEW ground motion prediction, and it may be recognized to be significantly large (never below 0.45), at least in this example. This means that alarming decisions based on this approach may be taken in very uncertain conditions, and this is because of the *IM* given *M* and *R* PDF (i.e., the GMPE). In fact, in the figure the *CoV* is computed, using Eq. (3), at any 1 s step from the earthquake origin time, in the following cases:

(a) considering both PDFs of *M* and *R*;
(b) considering the PDF of *M* and only the modal value of the distance (R^*) from Fig. 2d in place of its full PDF; and
(c) neither the PDF of *M* nor of *R*, while using two statistics as the mode of *R* and the maximum likelihood value of magnitude ($\overline{M}$).

Case (a) corresponds to fully apply the RTPSHA approach; in case (b) only the uncertainty on *M* reflects on the real-time *PGA* prediction; and in (3) neither uncertainty related to the estimation of *M* nor of *R* affects the estimation of *PGA*, and at any instant, the real-time hazard is simply given by $f_{PGA|M,R}(PGA|\overline{M},R^*)$. In this latter case the uncertainty is only that of the GMPE computed for the specific $\{\overline{M},R^*\}$ pair.

It clearly appears from the curves that the uncertainty of the distance is negligible with respect to the prediction of *PGA* because green and blue curves are overlapping, meaning that the *CoV* of *PGA* is almost the same with or without uncertainty on distance. Also the contribution of uncertainty on magnitude to the *CoV* of *PGA* is small if compared to that of the GMPE, except at the beginning when the estimation of *M* is not yet well constrained by several τ measurements. Unfortunately, the GMPE uncertainty, which largely dominates, is not dependent on the real-time measures involved in the described RTPSHA approach, and possible extensions and attempts reducing uncertainty in EEW ground motions predictions are discussed in Section 3.

Because of this time dependence of the *M* and *R* estimations, the prediction of *IM* becomes stable only after a number of stations have measured the early signal of the event. This is better shown in Fig. 6b where the estimation of the exceedance probability for three hypothetical PGA_c values, to be used in one of the decisional rules discussed, is given as a function of time (note that *t* equal to 7, 13 and 18 s corresponds to Fig. 2(a)–(c), respectively). It appears that the probability of exceedance does not change after 10–13 s, independently of which PGA_c value is considered. In other words, after on average 11–18 stations of the ISNet have measured τ, the estimation of the critical *PGA* does not benefit much from further information.

It may be concluded that there is a trade-off between the lead-time and the level of information based on which the alarm issuance is decided. Consequently, different lead-times may be computed for the Campania region, each of those corresponding to a different number of stations providing τ, for example, 4, 18 and 29 representing three levels of information about the source of the earthquake: *poor*, *large* and *full*, respectively; see [14] for details. Results in forms of maps are given in Fig. 7, and because they were computed considering as possible hypocenters those randomly occurring in the volume below the ISNet sensors up to a 12 km depth, in the maps minimum, maximum and average lead-time values are given. Because 18 stations are the minimum level of information to stabilize the uncertainty, the 18-station average lead-time map can be considered as the reference for the design of real-time risk reduction actions; some of which from [22] are superimposed in Fig. 8.

3. Envision of random field RTPSHA extensions

It has been discussed how GMPE carries the most of uncertainty in the estimation of ground motion parameters via the RTPSHA approach. In this section a preliminary and brief discussion of possible ways to include other data to improve the *IM* predictions and reduce associated uncertainty is sketched. They are mostly based on the information given by a correlation model for ground motion data and/or *IM*s measured at different sites and, in principle, allow for integration of regional/hybrid and on-site EEW systems.

3.1. Including information about IM measured at other sites

Consider the case of Fig. 9 in which the earthquake has reached one station at which the *IM* of interest (e.g., *PGA*) has been already measured (PGA_i), and assume the problem to solve is the same of Section 2, that is, predicting the peak ground acceleration at another site where the earthquake is not arrived yet (Fig. 9).

Studies (e.g., [16]) have shown that it is possible to assume the joint distribution of the logs of *PGA* at two sites as a bivariate

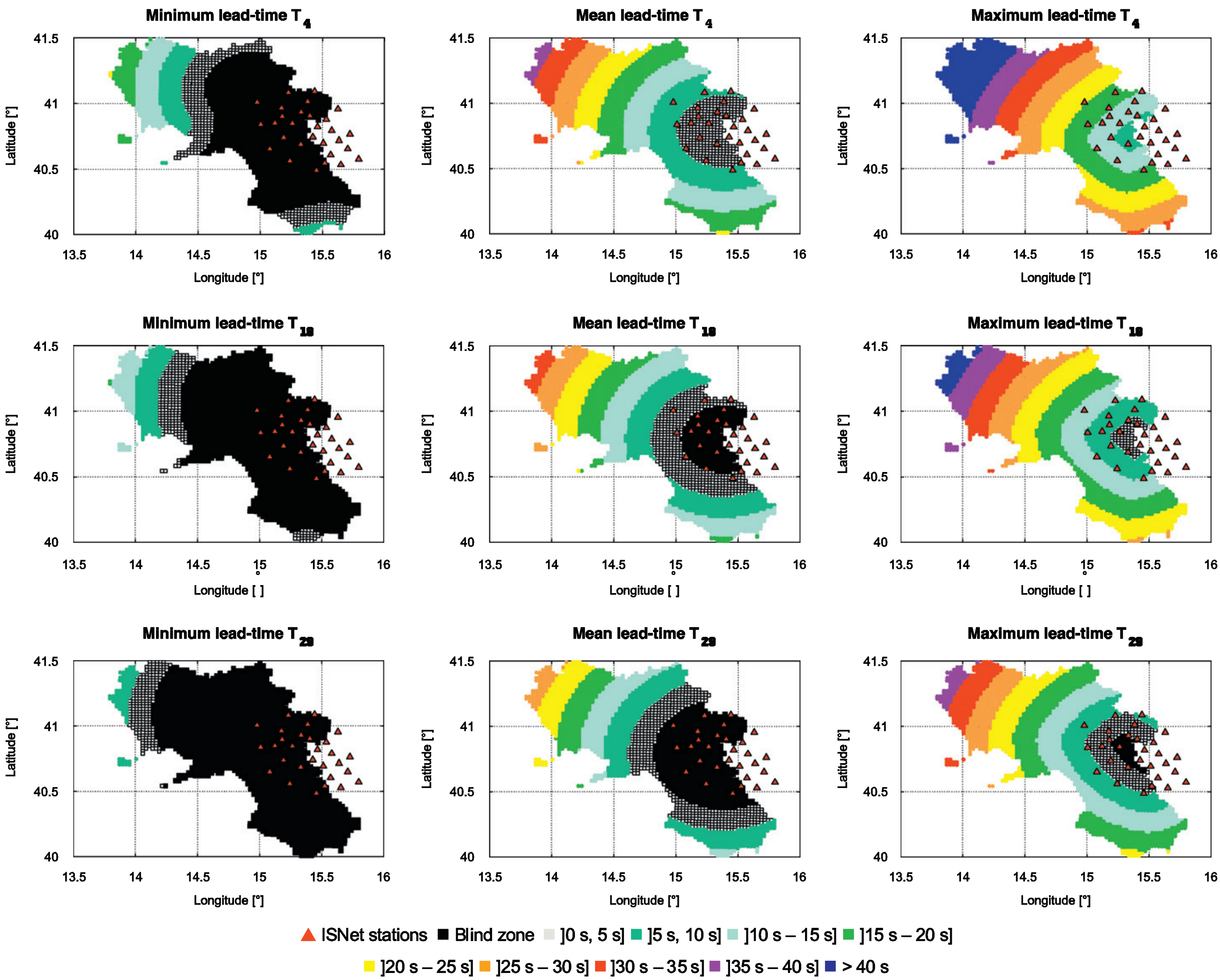

Fig. 7. Minimum, mean and maximum lead-time maps for random hypocenters when 4, 18 and 29 ISNet stations have provided information to estimate the magnitude.

Gaussian of mean vector and covariance matrix given in Eq. (8), where the mean is given by an GMPE (for example, that in [17] in which a, b, c, f and e are coefficients, the latter one depending on site conditions, S); and the covariance matrix is a function of the standard deviation of the residuals, σ, and the correlation coefficient, ρ, a function of the separation distance between the two sites i and j, $h_{i,j}$.

$$\begin{cases} \underline{\mu} = \begin{bmatrix} \mu_{\log(PGA_i)|M,R} \\ \mu_{\log(PGA_j)|M,R} \end{bmatrix} = \begin{bmatrix} a+b\,M+c\,\log\left(\sqrt{R_i^2+f^2}\right)+e\,S_i \\ a+b\,M+c\,\log\left(\sqrt{R_j^2+f^2}\right)+e\,S_j \end{bmatrix} \\ \underline{\underline{\Sigma}} = \sigma^2 \begin{bmatrix} 1 & \rho(h_{i,j}) \\ \rho(h_{i,j}) & 1 \end{bmatrix} \end{cases} \tag{8}$$

Then, the conditional distribution of the log of PGA_j, given the log of PGA_i, M and R, is still Gaussian, of parameters given in Eq. (9).

$$\begin{cases} \mu_{\log(PGA_j)|\log(PGA_i),M,R} = \mu_{\log(PGA_j)|M,R} + \rho(h_{i,j})[\log(PGA_i) - \mu_{\log(PGA_i)|M,R}] \\ \sigma_{\log(PGA_j)|\log(PGA_i)} = \sigma\sqrt{1-[\rho(h_{i,j})]^2} \end{cases} \tag{9}$$

Therefore, if one wants to compute the distribution of PGA_j given PGA_i, he can do that via the integral of Eq. (10) where it is assumed that the other data allow to estimate the magnitude of the earthquake and the distance of the two sites (i.e., the location of the earthquake). Then, the PDF of PGA_i also depends on such data. Moreover, rigorously, the PGA_i information should be used to better constrain the magnitude prediction as it carries information about M, i.e., $f(M|\underline{\tau},PGA_i)$ should be somehow available; on the other hand if it is possible to assume that $f(M|\underline{\tau},PGA_i) = f(M|\underline{\tau})$, and Eq. (10) may be solved with already available tools.

$$f(PGA_j|PGA_i,\underline{\tau},\underline{s}) = \int_m \int_{r_i} \int_{r_j} f(PGA_j|PGA_i,m,r_i,r_j)\, f(m|\underline{\tau},PGA_i)\, f(r_i|\underline{s})\, f(r_j|\underline{s})\, dm\,dr \tag{10}$$

Re-arranging the mean in Eq. (9) to highlight the correlation coefficient, Eq. (11), in which the same site conditions for i and j have been assumed, is obtained.

$$\mu_{\log(PGA_j)|\log(PGA_i),M,R} = (1-\rho)(a+b\,M+e\,S) + c\left[\log\left(\sqrt{\frac{R_j^2+f^2}{(R_i^2+f^2)^\rho}}\right)\right] + \rho\,\log(PGA_i) \tag{11}$$

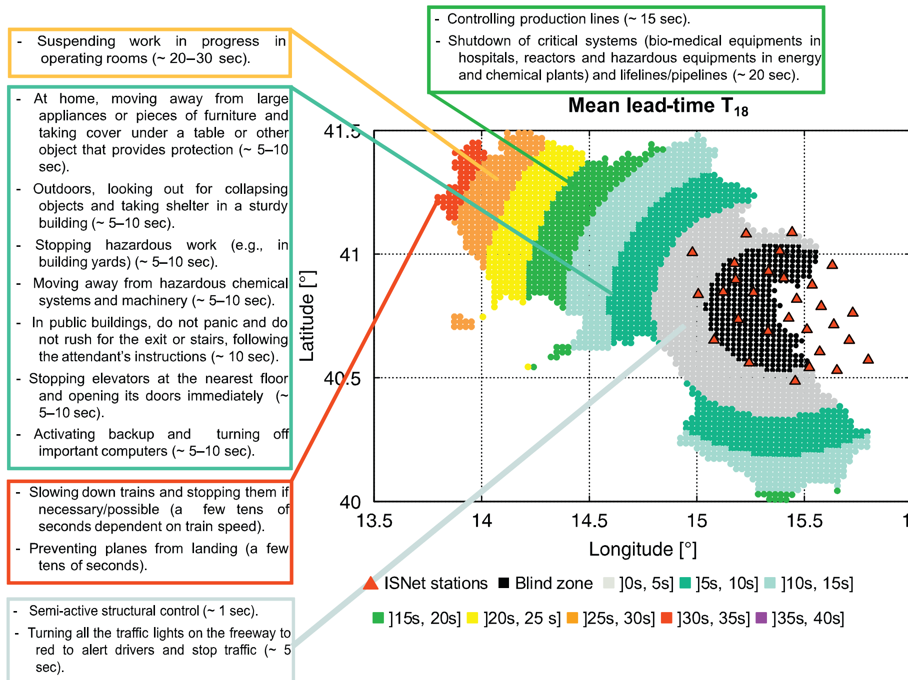

Fig. 8. Design lead-time map for the Campania region (southern Italy), modified from [14].

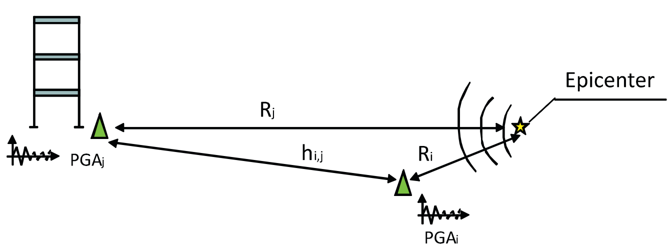

Fig. 9. EEW scheme when an *IM* measure is available at a station different from the site of interest.

It is to note that when the correlation is about perfect (ρ close to 1) and the two stations have the same distance from the source, M and R do not affect PGA_j so their estimation is useless; in this case PGA_j is about equal to PGA_i because the separation distance is almost zero. Conversely, when the correlation is zero, at large separation distances, PGA_i does not affect the PDF of PGA_j, i.e., PGA_j is independent of PGA_i. If the correlation between peak ground motion vanishes at, say $h_{i,j}$=40 km, beyond that limit knowing PGA_i is useless and only M and R matter for the estimation of PGA_j, as in the RTPSHA approach.

As an example of how the added PGA_i information may affect the estimation of PGA_j, in Fig. 10, three cases are shown for two stations, i and j, for one of which the PGA is already available. The example refers to an M 6 event for which the measured PGA_i at 15 km from the epicenter is 0.22 g (i.e., one half standard deviation above the mean for that M and R pair). In the cases shown the two stations are distant so that: (i) $h_{i,j}$=10 km, (ii) $h_{i,j}$=20 km and (iii) $h_{i,j}$=30 km. The corresponding values of the correlation coefficient are ρ=0.3, 0.1 and 0.03, respectively, computed via the arbitrary exponential correlation model $\rho(h)=1-e^{-4.7/40h}$, which is conservative for the correlation (i.e., intra-event residuals are expected to become uncorrelated much sooner in actual earthquakes, e.g., [18]).

It emerges the correlation becomes very weak soon after 10 km of separation distance, which means less than 3 s for the S-waves to travel from site i to site j, if a 3.5 km/s velocity is assumed; this means adding this information may not be practical for EEW purposes reducing significantly the available lead-time. Finally, it is to note that PGA_i is to be intended as the peak acceleration when the earthquake has ended, which raises the problem of determining when the measured PGA is final, a time when the S-waves may already have reached site j if $h_{i,j}$ is small (i.e., when the correlation is still significant).

3.2. Including information about IM predicted at other sites

Assume that at a site i it is possible to measure, in the early part of the signal, an observable d_i that is related to the final (unknown) peak ground acceleration (PGA_i) (Fig. 11), e.g., as discussed in [23]. Assume also that the distribution of the log of PGA_i, given d_i, may be defined.

Then an estimate of the final acceleration at site j may be obtained as in Eq. (12), in which it has been assumed that, given d_i, PGA_i does not depend on M and R or $f(PGA_i|d_i,M,R_i)=f(PGA_i|d_i)$ and that given PGA_i, PGA_j does not depend on d_i. However, PGA_j is conditional also on d_i and not only on τ, which requires, in principle, to be able to estimate M on the basis of the different measures at the same time.

$$f(PGA_j|d_i,\underline{\tau},\underline{s}) = \int_m \int_{PGA_i} \int_{r_i} \int_{r_j} f(PGA_j|PGA_i,m,r_i,r_j)\, f(PGA_i|d_i)\, f(m|d_i,\underline{\tau}) \times f(r_i|\underline{s})\, f(r_j|\underline{s})\; d(PGA_i)\, dm\, dr \qquad (12)$$

Alternatively, if a single parameter is available to estimate both M and PGA_i, the PDF of the latter may be computed as

$$f(PGA_j|d_i,\underline{s}) = \int_m \int_{PGA_i} \int_{r_i} \int_{r_j} f(PGA_j|PGA_i,m,r_i,r_j)\, f(PGA_i|d_i) \times f(m|d_i)\, f(r_i|\underline{s})\, f(r_j|\underline{s})\; d(PGA_i)\, dm\, dr \qquad (13)$$

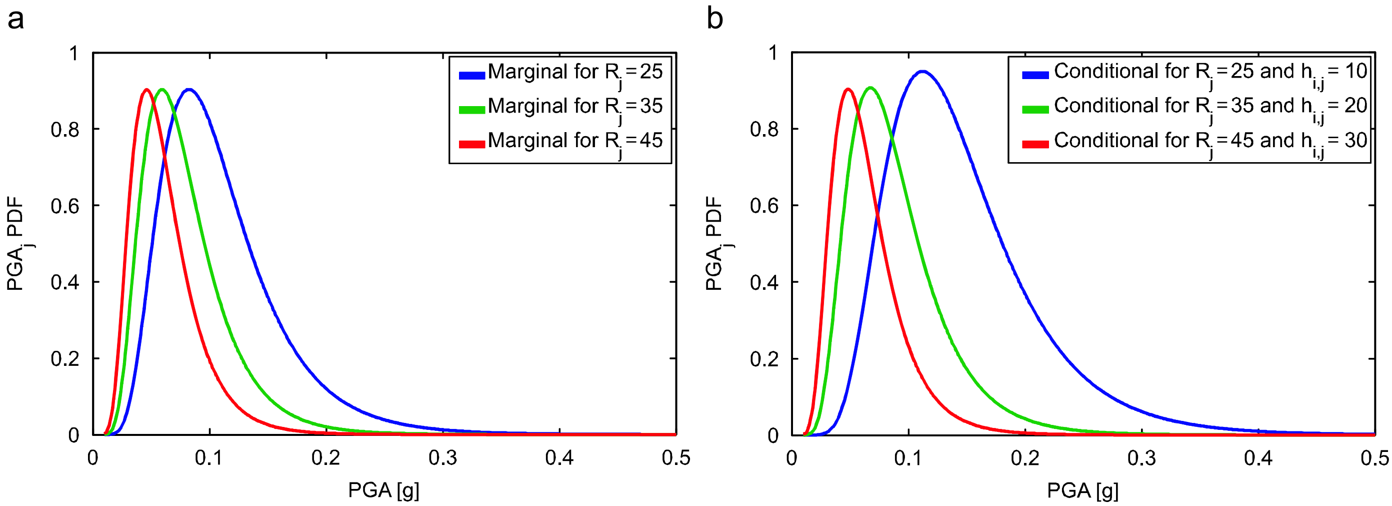

Fig. 10. PDFs of PGA_j given only M and R (a) and conditional PDFs of PGA_j given M, R and PGA_i for three possible values of separation distance between stations i and j.

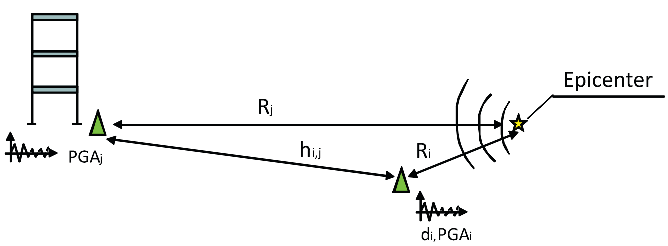

Fig. 11. EEW scheme when an additional parameter to estimate the *IM* local at a station different from the site of interest is available.

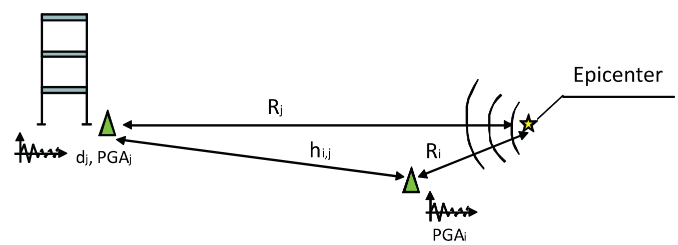

Fig. 12. EEW scheme when an *IM* measure is available at a station different from the site of interest and an additional parameter to estimate the *IM* local at the site of interest are available.

3.3. Improving on-site EEW

The third case considered here is when the on-site warning approach (i.e., when a parameter read on the P-waves at a station is used to predict the final *PGA* at that same site) is integrated with information read somewhere else, Fig. 12, if it is believed to be beneficial for the estimation. In this case, the sought distribution is $f(PGA_j|d_j,PGA_i)$, in which the dependence on $\underline{s}$ has been neglected for simplicity, assuming that the distance between the sites i and j is small and only local measures count (i.e., $f(PGA_j|d_j,PGA_i,m,r)=f(PGA_j|d_j,PGA_i)$) it may be retrieved as in Eq. (14).

$$f(PGA_j|d_j,PGA_i)=f(PGA_j,d_j,PGA_i,m,r)/f(d_j,PGA_i,m,r) \tag{14}$$

4. Estimating earthquake consequences for structures in real-time

The real-time prediction of a ground motion *IM* discussed so far, although the first step from real-time seismology to structural performance, is neither the best option to estimate the damage potential for a specific structure nor the more appropriate piece of information on the basis of which to decide whether to alarm. In fact, it is well known that the *IM* maybe only poorly correlated to the structural seismic response and that different damages occurring in a building (e.g., to structural components, to non-structural components and to content) may require the estimation of more than one *IM* at the same time. In other words, if one is able to quantify the damages (i.e., the loss) specific for the structure of interest, this is a sounder basis for the warning management. This structure-specific EEW design procedure was investigated in [11] where it was shown with respect to the issue of calibrating an alarm threshold, which is *optimal* in the sense of minimizing the losses, including the false and missed alarm related costs. Such an approach is briefly reviewed in the following.

The performance-based seismic risk assessment of structures aiming to the estimation of the mean annual frequency of certain loss (L) may be adapted to the EEW real-time case as done for the RTPSHA. In fact, for a structure provided of an EEW system such as ERGO (Section 2.3), the expected loss may be computed in the case of warning issuance (W) and no warning issuance ($\overline{W}$) as follows:

$$E^W[L|\underline{\tau},\underline{s}]=\int_L\int_{DM}\int_{EDP}\int_{IM} l f^W(l|\underline{dm})\, f(\underline{dm}|\underline{edp})\, f(\underline{edp}|\underline{im}) \times f(\underline{im}|\underline{\tau},\underline{s})\; dL\;\; d\underline{DM}\; d\underline{EDP}\;\; d\underline{IM} \tag{15}$$

$$E^{\overline{W}}[L|\underline{\tau},\underline{s}]=\int_L\int_{DM}\int_{EDP}\int_{IM} l f^{\overline{W}}(l|\underline{dm})\, f(\underline{dm}|\underline{edp})\, f(\underline{edp}|\underline{im}) \times f(\underline{im}|\underline{\tau},\underline{s})\; dL\;\; d\underline{DM}\;\; d\underline{EDP}\;\; d\underline{IM} \tag{16}$$

where the terms the two equations share are: $f(l|\underline{dm})$, which is the PDF of the loss given the vector of damage measures ($\underline{DM}$); $f(\underline{dm}|\underline{edp})$ or the joint PDF of damages given the engineering demand parameters ($\underline{EDP}$), proxy for the structural response; $f(\underline{edp}|\underline{im})$ or the joint PDF of the *EDP*s generally conditional to a vector of ground motion intensity measures ($\underline{IM}$); and $f(\underline{im}|\underline{\tau},\underline{s})$ is the real-time hazard for the $\underline{IM}$ vector.

The two equations are different for the loss function term. In other words, it may be assumed that a security action, aimed at risk mitigation, is undertaken if the alarm is issued. For example, some critical system will shut down or people in a school building may duck under desks if the warning time is not sufficient to evacuate (more complex security measures may be related to the semi-active control of buildings; see Section 5). In fact, $f^{W}(l|\underline{dm})$ is the loss reflecting the risk reduction, and $f^{\overline{W}}(l|\underline{dm})$ is the loss function if no alarm is issued (no security action is undertaken).

In the case it is possible to compute, before the ground motion hits, the expected losses in case of warning or not, clearly one can take the optimal decision: to alarm if this reduces the expected losses and to not issue any warning otherwise:

$$\begin{cases} \text{to alarm if} & E^{W}[L|\underline{\tau},\underline{s}] \le E^{\overline{W}}[L|\underline{\tau},\underline{s}] \\ \text{to not alarm if} & E^{W}[L|\underline{\tau},\underline{s}] > E^{\overline{W}}[L|\underline{\tau},\underline{s}] \end{cases} \tag{17}$$

The described approach was pursued for a simplified school building consisting of one classroom (Fig. 1), in which three kinds of losses were considered, the assumed occurrence of which is summarized in Table 2.

The costs of casualties and injuries were conventionally assigned in an approach similar to insurance premiums' computation. The security action to be undertaken after the alarm issuance was supposed to be ducking of occupants under desks.

To reflect the undertaking of the security action in case of alarm, the loss function was generally reduced with respect to the non-issuance alarm case (Fig. 14a). All other terms shared by Eqs. (15) and (16) were computed via non-linear structural analyses.

With this approach $E^{W}[L|\hat{\tau}]$ and $E^{\overline{W}}[L|\hat{\tau}]$ were calculated for the example under exam considering the ISNet EEW system, for 10 equally spaced $\hat{\tau}$ values in the range between 0.2 and 2 s and assuming $n=29$, i.e., it is assumed that all stations of the ISNet have measured τ. Because it has been discussed that the localization method involves negligible uncertainty, the R value has been fixed to 110 km, which is a possible distance of a building in Naples for an event having its epicentral location in the Irpinian region. In Fig. 14b the trends of the expected losses in the two cases are given: the black curve (dashed and solid) corresponds to the non-issuance of the alarm and the red one refers to the issuance. The intersection of the two curves defines two $\hat{\tau}$ regions and the optimal alarm threshold ($\hat{\tau}_W$); if the statistic of the measurements is below the intersection value the expected loss is lower if the warning is not issued, otherwise, if $\hat{\tau} > \hat{\tau}_W$, the optimal decision is to alarm because it minimizes the expected loss.

To determine the alarm threshold based on the expected loss allows to account for all actual costs related to the event striking and the alarm consequences probabilistically, and it is easy to recognize how this is an improvement with respect to synthesize all structural response, damages and consequences in the im_c threshold discussed above. Moreover, because the loss estimations account for false and missed alarms, the threshold is also optimal with respect to the *MA* and *FA* tradeoff.

5. Possible yet limited interaction of EEW and structural control

The most advanced EEW application engineers can think of is structural control, i.e., using the early information to better prepare the structure to respond to the earthquake. The three main classes of control systems are: (1) *passive*, (2) *active* and (3) *semi-active* [24].

(1) A passive control system is based on the motion of the structure to develop the control force and usually does not require an external power source to operate (i.e., seismic base isolation). Passive systems need to be designed according to a scenario of the seismic action. Then, it is hard to attempt integrating EEWS with passive control systems.
(2) An active control system supplies control forces based on feedback from sensors (located on the structure) that measure the excitation and/or the actual response. The recorded measurements from the response and/or excitation are monitored by a controller, which operates the actuators producing the forces. Typical active control strategies are based on information about the seismic input which cannot be predicted by the described EEWS.
(3) A semi-active (SA) system develops control forces based on the feedback from sensors that measure the excitation and/or the response of the structure. However, the control forces are not realized, as in the active case, by actuators, but rather by modifying, possibly in real-time, the characteristics of special devices (SA links). The energy required for the modification of the basic parameters of the devices may be furnished even by batteries (e.g., to open/close of valve). For these reasons, SA control strategies seem to have at least the potential to seismic protection of structures and infrastructure in combination with an EEWS [25,26].

5.1. Fluid viscous dampers for EEW-based semi-active structural control

One means of achieving a semi-active damping device is to use a controllable valve to alter the resistance to flow of a conventional hydraulic fluid damper. Semi-active fluid viscous dampers typically consist of a hydraulic cylinder containing a piston head that separates the two sides of the cylinder. As the piston is cycled, the fluid within the damper (usually oil) is forced to pass through small orifices. The output force is modulated by an external control valve, which connects the two sides of the cylinder. If the device is characterized only by two states (e.g., the valve can only be open or closed) the system is referred to as an ON–OFF SA system, otherwise if the mechanical parameter of the device can assume any value in a certain range (e.g., the valve opens and closes gradually) the system is referred to as a continuous SA system.

Table 2
Losses considered and occurrence cases.

Loss	Structural collapse	Non-structural damage only	Neither structural nor non-structural damage
Cost due to casualties and injuries	Occurs	May occur (in a reduced manner in the case of warning)	Does not occur
Cost due to structural reparation and re-construction	Occurs	Does not occur	Does not occur
Cost related to downtime	Occurs	Occurs	Occurs in the case of warning

Although more complex models are available, the dynamic behavior of fluid dampers may be described based on a simple model consisting of a linear viscous dashpot with a voltage-dependent damping coefficient, $C_{SA}(u)$. The force output, F, is thus described by

$$F = C_{SA}(u)\dot{x} \tag{18}$$

where $\dot{x}$ is the relative velocity of the piston with respect to the damper housing and u is the command voltage. The damping coefficient of Eq. (18) increases if the voltage decreases and it is bounded by minimum and maximum values corresponding to the open and closed valve positions, respectively, Eq. (19). The response time for modifying the variable damper from high-to-low or low-to-high damping is generally less than 30 ms and then compatible with very short lead-time.

$$\begin{cases} \text{valve closed} \Leftrightarrow C_{SA}(u) = c_{max} \\ \text{valve open} \Leftrightarrow C_{SA}(u) = c_{min} \end{cases} \tag{19}$$

In the EEW prospective, once an uncontrolled structural response prediction (EDP_u) for a structure of interest is available, a decisional condition has to occur to issue the alarm (i.e., to activate the device). For example, the device may be activated if the expected value, $E[EDP_u|\underline{\tau},\underline{s}]$, of the structural response variable exceeds a critical threshold (EDP_c), Eq. (20). The expected value of the chosen EDP may be computed as in Eq. (21).

$$\begin{cases} C_{SA}(u) = c_{max} & \text{if} \quad E[EDP_u|\underline{\tau},\underline{s}] \geq EDP_c \\ C_{SA}(u) = c_{min} & \text{if} \quad E[EDP_u|\underline{\tau},\underline{s}] < EDP_c \end{cases} \tag{20}$$

$$E[EDP_u|\underline{\tau},\underline{s}] = \int_{EDP}\int_{IM} edp_u\, f(edp_u|im)\, f(im|\underline{\tau},\underline{s})\, d(edp_u)\, d(im) \tag{21}$$

As an example, let us consider the same simple structure of Fig. 13a now equipped with a bracing system including variable viscous dampers operating in ON–OFF SA mode (Fig. 15a). It can be modeled as a T=0.6 s single degree of freedom (SDOF) system with an elastic–perfectly-plastic behavior and a yielding moment of 200 kNm. In the uncontrolled configuration, the semi-active damper has the control valve fully open, and thus the damper produces no control force. In the controlled configuration, the control valve is held fixed in the closed position (i.e., in a high damping configuration).

The considered EDP related to structural damage is the interstorey drift ratio (IDR) as a function of the PGA. As an additional EDP, which may be of concern in the case one is interested in the response of non-structural elements, the peak floor acceleration (P_{FA}) was also considered. The expected values of the chosen EDPs were computed as a function of the information provided in

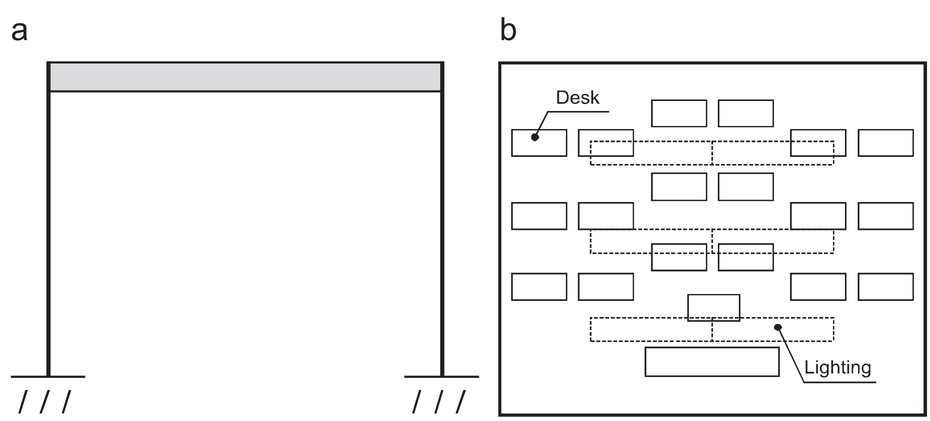

Fig. 13. Structural scheme for the school building (a) and classroom layout (b), modified from [11].

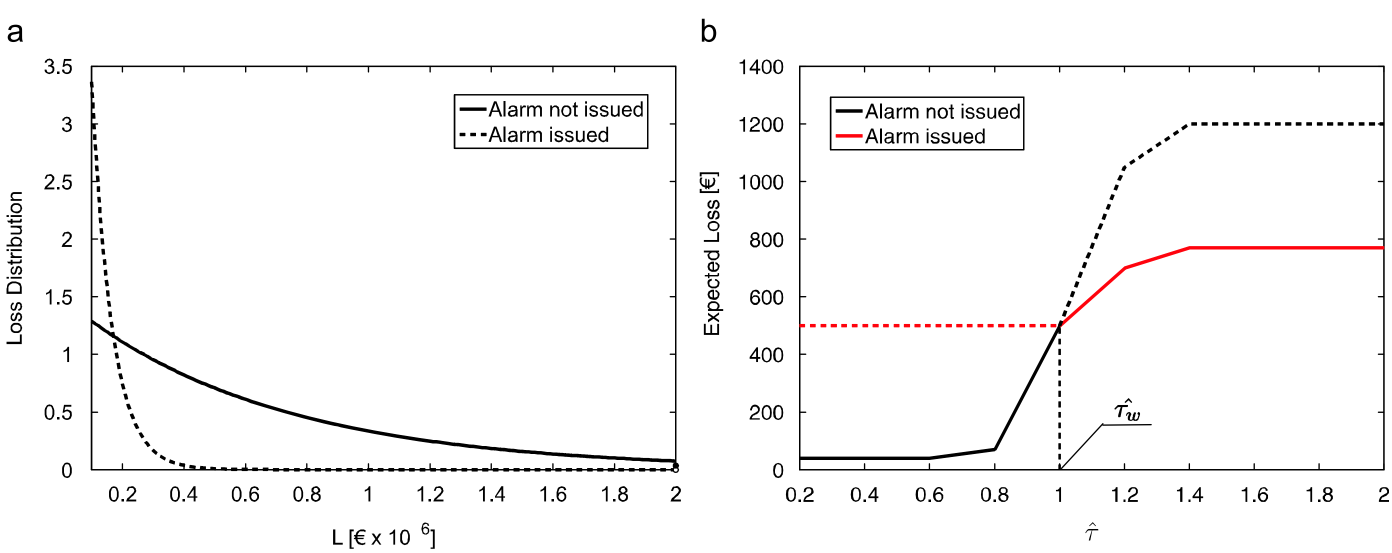

Fig. 14. Loss PDF when the alarm is not issued and when it is reduced because ducking under desks after the alarm is issued (a) and expected loss as a function of the measures used to estimate the magnitude in real-time with identified optimal alarm threshold (b), modified from [11].

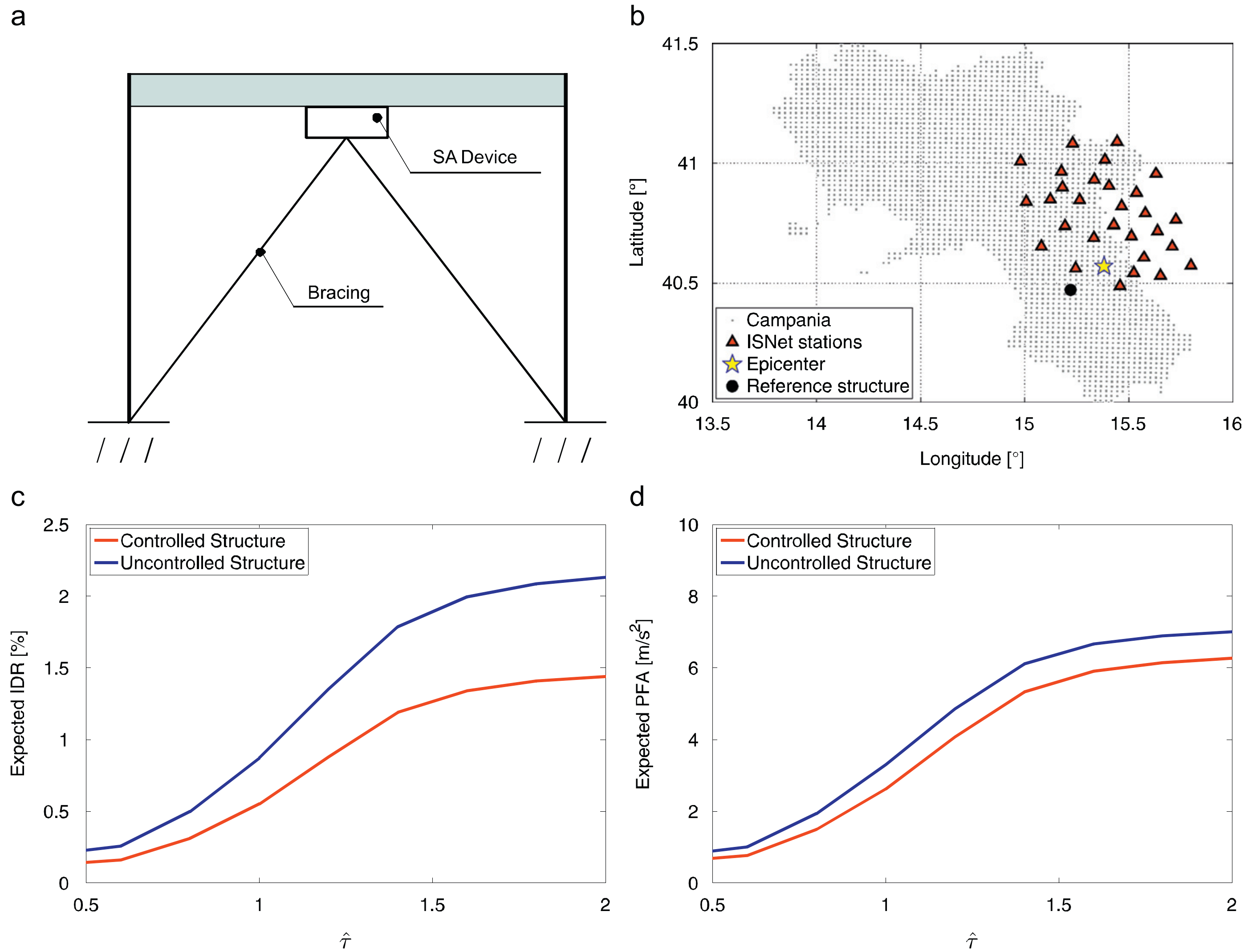

Fig. 15. Structural scheme for the controlled building (a), ISNet and possible location of the structure (b), comparison between the expected IDR (c) and the expected P_{FA} (d) of controlled and uncontrolled structure as a function of the statistics of the network measurements (adapted from [25]).

real-time by the EEWS. To this aim it was supposed that the structure is in the Irpinia region at 10 km (in terms of epicentral distance) with respect to the location of an hypothetical earthquake occurring within the ISNet (Fig. 15b) and therefore with a very limited available lead-time (according to Fig. 7).

The expected values of both IDR and P_{FA} were computed for 11 equally spaced $\hat{\tau}$ values in the range between 0.5 and 2 s. All the analyses are conditional to the fact that the level of information provided by the EEWS corresponds to 18 stations, e.g., 18 measures of τ are available. Moreover, the R-value has been deterministically fixed to 10 km. Results of the analyses are presented in Fig. 15c and d. The curves represent the trends of the *EDPs* for the specific structure at the given location. They provide the mitigation of structural response eventually given by the structural control, with respect to the uncontrolled structure, in the case of different earthquakes represented by specific $\hat{\tau}$ values.

It is finally to underline that, despite the described analyses that are only a very preliminary attempt, the effectiveness of structural control activated by an EEW system has to be proven with respect to traditional control strategies. In fact, it should be proven that activating the system via the EEW is better than having a conventional control system or a passive system, e.g., because the control system runs on batteries and therefore cannot be continuously operating, or because it is proven that the information about the impending earthquake provided by the EEW system may be used to fruitfully adjust in real-time the properties of the control devices to improve the structural response with respect to passive systems. This may require the EEW system is able to predict in real-time the frequency content of the incoming ground motion; this is more difficult, and although some attempt exists [27], to date, it is not feasible by RTPSHA, in which the spectral shape is a static piece of information given by the GMPE.

6. Conclusions

In this paper a performance-based earthquake engineering framework to earthquake early warning was reviewed. The focus is the probabilistic prediction of the structural consequences or losses at a given site based on the information gathered during an earthquake by a seismic network able to process in real-time the recordings.

The first step was the early warning adaption of probabilistic seismic hazard analysis, which allows to predict in real-time any ground motion intensity measure for which a prediction equation is available. As a side result, an analytical form solution for the real-time estimation of magnitude, under some hypotheses, was found based on some fundamental results of real-time seismology. Subsequently, the alarm issuance based on strong motion intensity measures was faced. Possible decisional rules and consequent missed and false alarm probabilities were analyzed.

In the context of site-specific engineering ground motion predictions, it was shown that the GMPE is the largest source of uncertainty with respect to real-time estimate of source parameters as magnitude and location. Similarly, it was shown that because in EEW systems the uncertainty is time-dependent, it may be identified a time after which the level of information does not increase significantly, although the earthquake has not yet reached all stations within the network. Therefore uncertainty-dependent lead-time should be considered as an additional design parameter for engineering EEW applications.

On one seismological side, the proposed real-time seismic risk analysis approach may be extended to include more information to estimate source parameters and ground motion at other sites. This may be an opportunity to reduce the uncertainty in EEW predictions; however, this may require to model the spatial correlation of ground motion and the setup of multiple relationships between real-time observables and parameters to be predicted.

On the structural engineering counterpart, in principle, the structural performance and losses may be predicted in real-time, which allow to evaluate the actual efficiency of security actions, to account explicitly for the cost of false alarms and to take the alarming decision on a more rational basis for a specific structure, i.e., based on expected losses.

The preliminary exploration of the possible automated interaction of EEW and structural control was also discussed. This is a pioneering topic in EEW and still requires advancements in both the real-time seismology and earthquake engineering.

Finally, from this brief review of a possible design approach to structure-specific EEW it emerges that many important issues in engineering earthquake early warning still need to be addressed: first of all the effectiveness with respect to more traditional structural seismic risk mitigation technologies. However, these studies at least prove that EEW deserves attention from earthquake engineering among advanced cost-effective risk management approaches.

Acknowledgements

The author would like to explicitly express his gratitude to Massimiliano Giorgio for his essential contribution to all the studies presented and also to Gaetano Manfredi, Paolo Gasparini, the RISSC Lab group and, among students, Carmine Galasso. Most of the research presented in this paper was developed within the funded research programs of AMRA (http://www.amracenter.com/) and the ReLUIS-DPC 2005–2008 project.

References

[1] Heaton TH. A model for a seismic computerized alert network. Science 1985;228(4702):87–90.
[2] Kanamori H. Real-time seismology and earthquake damage mitigation. Annual Review of Earth and Planetary Sciences 2005;3(5.1–):5.20.
[3] Veneziano D, Papadimitriou AG. Optimization of the seismic early warning system for the Tohoku Shinkansen. In: Proceedings of the 11th European conference on earthquake engineering, Paris, France; 1998.
[4] Wieland M, Griesser M, Kuendig C. Seismic early warning system for a nuclear power plant. In: Proceedings of the 12th world conference on earthquake engineering, Auckland, New Zealand; 2000.
[5] Wieland M. Earthquake alarm, rapid response, and early warning systems: low cost systems for seismic risk reduction. Zurich, Switzerland: Electrowatt Engineering Ltd.; 2001. Available at 〈http://www.gadr.giees.uncc.edu/DOCS/Theme_A_sent_oct_15/7.%20BLUEPRINT%20A.7%20MARTIN%20WIEILAND.doc〉.
[6] Wald JD, Quitoriano V, Heaton TH, Kanamori H, Scrivner CW, Orden BC. TriNet "ShakeMaps": rapid generation of peak ground motion and intensity maps for earthquake in Southern California. Earthquake Spectra 1999;15(3):537–55.
[7] Doi K.The operation and performance of earthquake early warnings by the Japan Meteorological Agency. Soil Dynamics and Earthquake Engineering (this issue). doi:10.1016/j.soildyn.2010.06.009.
[8] Iervolino I, Convertito V, Giorgio M, Manfredi G, Zollo A. Real time risk analysis for hybrid earthquake early warning systems. Journal of Earthquake Engineering 2006;10(6):867–85.
[9] Cornell CA, Krawinkler H. Progress and challenges in seismic performance assessment. PEER Center News 2000;3(2):4.
[10] Cornell CA. Engineering seismic risk analysis. Bulletin of the Seismological Society of America 1968;58(5):1583–606.
[11] Iervolino I, Giorgio M, Manfredi G. Expected loss-based alarm threshold set for earthquake early warning systems. Earthquake Engineering and Structural Dynamics 2007;36(9):1151–68.
[12] Allen RM, Kanamori H. The potential for earthquake early warning in Southern California. Science 2003;300(5620):786–9.
[13] Convertito V, Iervolino I, Manfredi G, Zollo A. Prediction of response spectra via real-time earthquake measurements. Soil Dynamics and Earthquake Engineering 2008;28(6):492–505.
[14] Iervolino I, Giorgio M, Galasso C, Manfredi G. Uncertainty in early warning predictions of engineering ground motion parameters: what really matters? Geophysical Research Letters 2009;36:L00B06, doi:10.1029/2008GL036644.
[15] Satriano C, Lomax A, Zollo A. Real-time evolutionary earthquake location for seismic early warning. Bulletin of the Seismological Society of America 2008;98(3):1482–94.
[16] Jayaram N, Baker JW. Statistical tests of the joint distribution of spectral acceleration values. Bulletin of the Seismological Society of America 2008;98(5):2231–43.
[17] Sabetta F, Pugliese A. Estimation of response spectra and simulation of nonstationarity earthquake ground motion. Bulletin of the Seismological Society of America 1996;86(2):337–52.
[18] Esposito S, Iervolino I, Manfredi G. PGA semi-empirical correlation models based on European Data. In: Proceedings of the 14th European conference on earthquake engineering, Ohrid, Republic of Macedonia; 2010.
[19] Weber E, Convertito V, Iannaccone G, Zollo A, Bobbio A, Cantore L, et al. An advanced seismic network in the southern Apennines (Italy) for seismicity investigations and experimentation with earthquake early warning. Seismological Research Letters 2007;78(6):622–34.
[20] Iervolino I, Manfredi G, Cosenza E. Earthquake early warning and engineering application prospects. In: Paolo Gasparini, Gaetano Manfredi, Jochen Szchau, editors. Earthquake Early Warning. Springer; 2007. ISBN:978-3-540-72240-3.
[21] Festa G, Martino C, Lancieri M, Zollo A, Iervolino I, Elia L, et al. ERGO: a visual tool for testing earthquake early warning systems (in preparation).
[22] Goltz JD. Introducing earthquake early warning in California: a summary of social science and public policy issues. In: Report to OES and the operational areas. Governor's Office for Emergency Service, Pasadena, CA, US; 2002. (Available at 〈http://www.cisn.org/docs/Goltz.TaskI-IV.Report.doc〉).
[23] Wu Y-M, Kanamori H. Rapid assessment of damage potential of earthquakes in Taiwan from the Beginning of P-waves. Bulletin of the Seismological Society of America 2005;95(3):1181–5.
[24] Symas MD, Constantinou MC. Semi-active control systems for seismic protection of structures: a state-of-the-art review. Engineering Structures 1999;21(6):469–87.
[25] Iervolino I, Galasso C, Manfredi G. Preliminary investigation on integration of semi-active structural control and earthquake early warning. Early Warning System for Transport Lines Workshop. KIT Science Report, Karlsruhe, Germany; 2010. ISSN:1619-7399.
[26] Fujita S, Minagawa K, Tanaka G, Shimosaka H, Intelligent seismic isolation system using air bearings and earthquake early warning. Soil Dynamics and Earthquake Engineering (this issue). doi:10.1016/j.soildyn.2010.06.006.
[27] Pnevmatikos NG, Kallivokas LF, Gantes CJ. Feed-forward control of active variable stiffness systems for mitigating seismic hazard in structures. Engineering Structures 2004;26(4):471–83.